

## Supporting Information for

### Synthesis, structure, and superconductivity of $\text{La}_{7+2x}\text{Sr}_{1-}$



Deyang Xu<sup>a</sup>, Guohong Cai<sup>b</sup>, Peiliang Huang<sup>c</sup>, Xi Wu<sup>d</sup>, Yan Wang<sup>b</sup>, Jinling Geng<sup>b</sup>,  
Jing Ju<sup>b</sup>, Xiaoge Wang<sup>b</sup>, Congling Yin<sup>a\*</sup>, Guobao Li<sup>b\*</sup>

*a. MOE Key Laboratory of New Processing Technology for Nonferrous Metals and Materials, Guangxi Key Laboratory of Optical and Electronic Materials and Devices, College of Materials Science and Engineering, Guilin University of Technology, Guilin 541004, People's Republic of China*

*b. Beijing National Laboratory for Molecular Sciences, State Key Laboratory of Rare Earth Materials Chemistry and Applications, College of Chemistry and Molecular Engineering, Peking University, Beijing, 100871, People's Republic of China*

*c. Beijing Ritan High School, Beijing, 100020, People's Republic of China*

*d. Henan Institute of Chemical Technology, Kaifeng, 475000, People's Republic of China*

\*E-mail: [conglings.yin@glut.edu.cn](mailto:conglings.yin@glut.edu.cn) (C.Y.), and [liguobao@pku.edu.cn](mailto:liguobao@pku.edu.cn) (G.L.)

1. Rietveld plot of the X-ray diffraction data of LSKNCO1, LSKNCO2, LSKNCO3, LSKNCO4, LSKNCO6, LSKNCO7, LSKNCO8, LSKNCO10, LSKNCO11, and Rietveld plot of the neutron diffraction data of LSKNCO2.

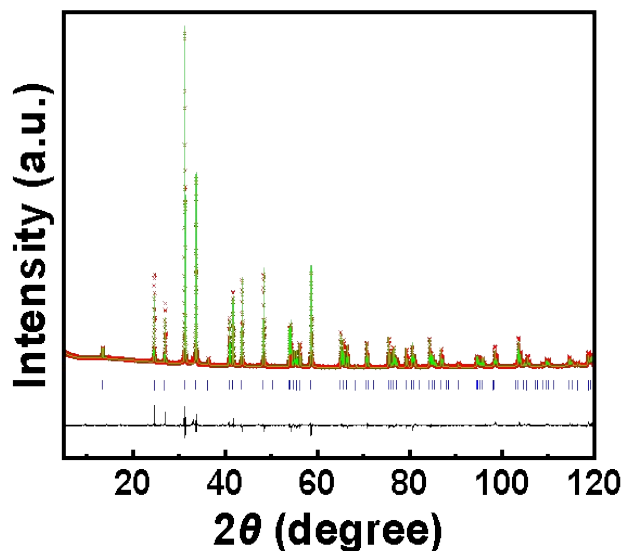


**Figure S1.** Rietveld plot of the X-ray diffraction data of LSKNCO1 at room temperature. The plus symbol represents the observed value, the solid line represents the calculated value, the marks below the diffraction patterns are the calculated reflection positions, and the difference curve is shown at the bottom in the figure.

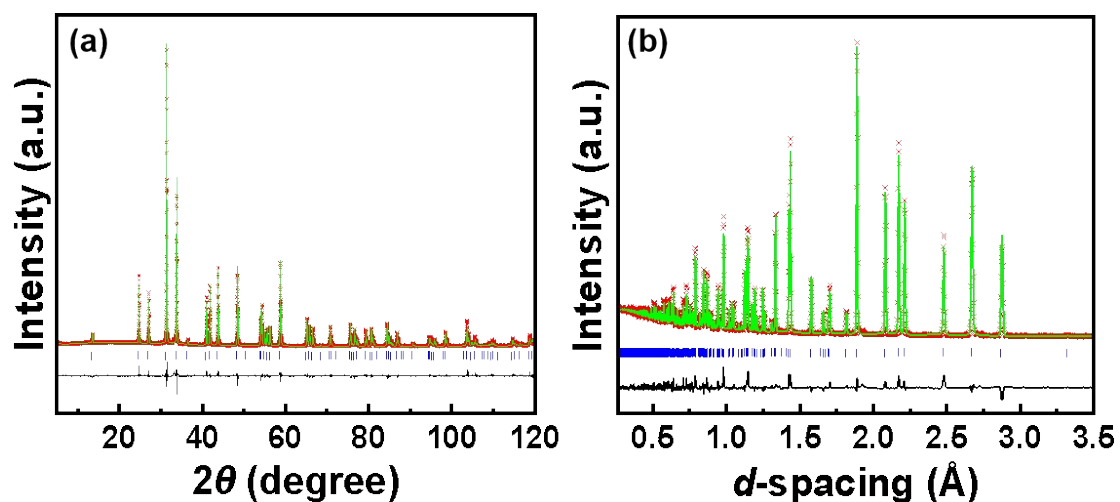


**Figure S2.** Rietveld plot of the X-ray (a) and neutron diffraction data (b) of LSKNCO2 at room temperature. The plus symbol represents the observed value, the solid line represents the calculated value, the marks below the diffraction patterns are the calculated reflection positions, and the difference curve is shown at the bottom in the figure.

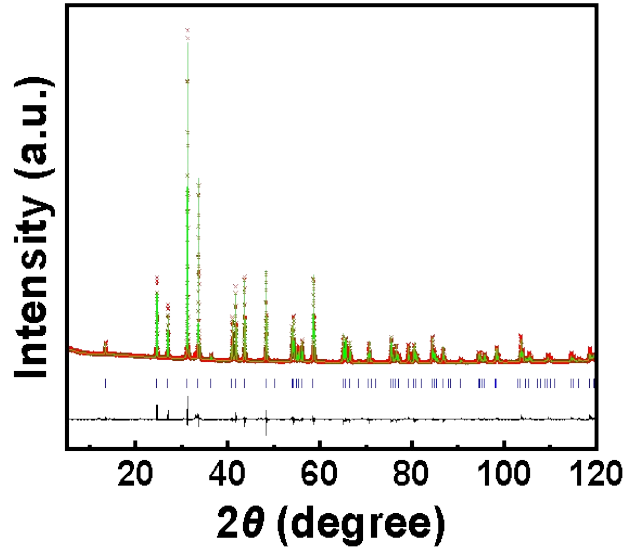


**Figure S3.** Rietveld plot of the X-ray diffraction data of LSKNCO<sub>3</sub> at room temperature. The plus symbol represents the observed value, the solid line represents the calculated value, the marks below the diffraction patterns are the calculated reflection positions, and the difference curve is shown at the bottom in the figure.

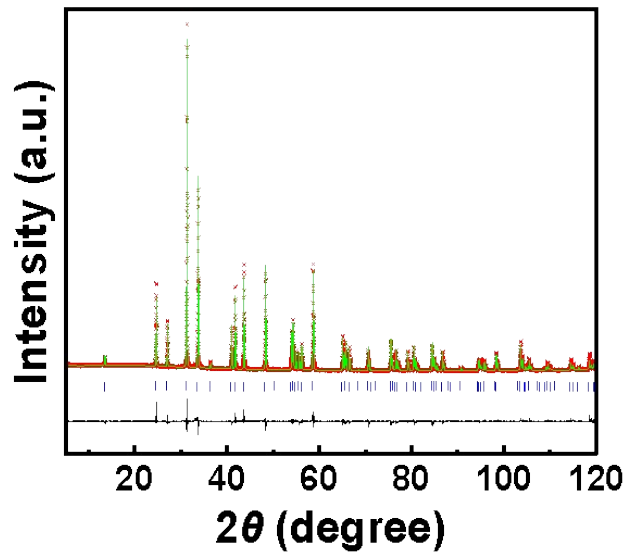


**Figure S4.** Rietveld plot of the X-ray diffraction data of LSKNCO<sub>4</sub> at room temperature. The plus symbol represents the observed value, the solid line represents the calculated value, the marks below the diffraction patterns are the calculated reflection positions, and the difference curve is shown at the bottom in the figure.

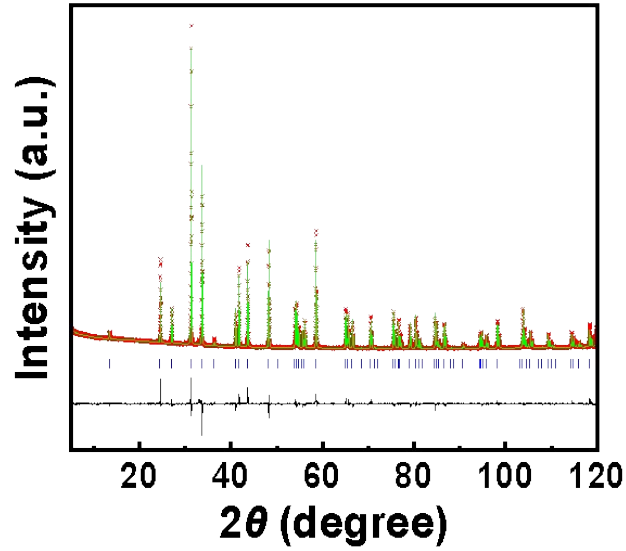


**Figure S5.** Rietveld plot of the X-ray diffraction data of LSKNCO6 at room temperature. The plus symbol represents the observed value, the solid line represents the calculated value, the marks below the diffraction patterns are the calculated reflection positions, and the difference curve is shown at the bottom in the figure.

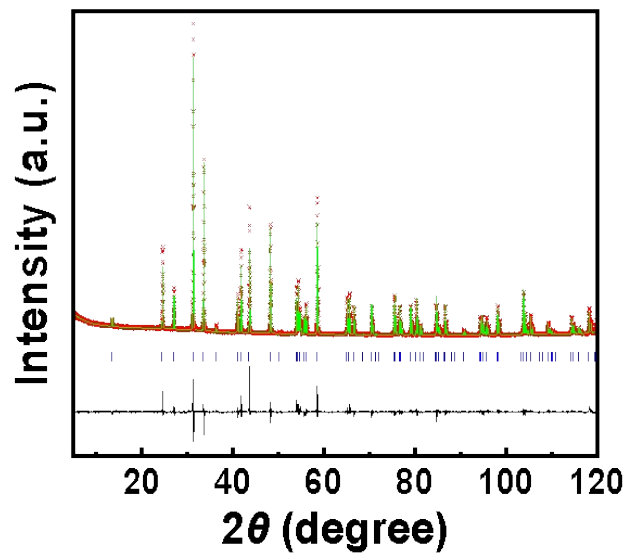


**Figure S6.** Rietveld plot of the X-ray diffraction data of LSKNCO7 at room temperature. The plus symbol represents the observed value, the solid line represents the calculated value, the marks below the diffraction patterns are the calculated reflection positions, and the difference curve is shown at the bottom in the figure.

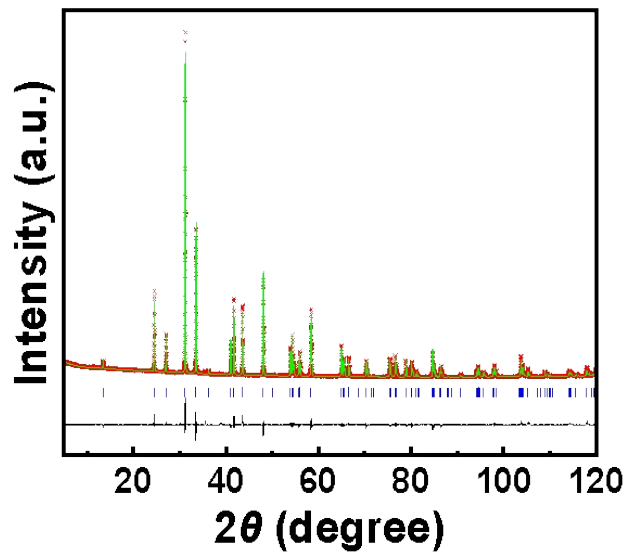


**Figure S7.** Rietveld plot of the X-ray diffraction data of LSKNCO8 at room temperature. The plus symbol represents the observed value, the solid line represents the calculated value, the marks below the diffraction patterns are the calculated reflection positions, and the difference curve is shown at the bottom in the figure.

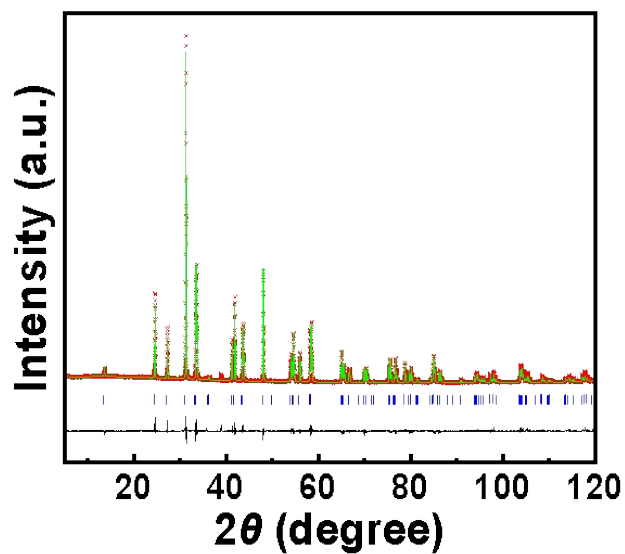


**Figure S8.** Rietveld plot of the X-ray diffraction data of LSKNCO10 at room temperature. The plus symbol represents the observed value, the solid line represents the calculated value, the marks below the diffraction patterns are the calculated reflection positions, and the difference curve is shown at the bottom in the figure.

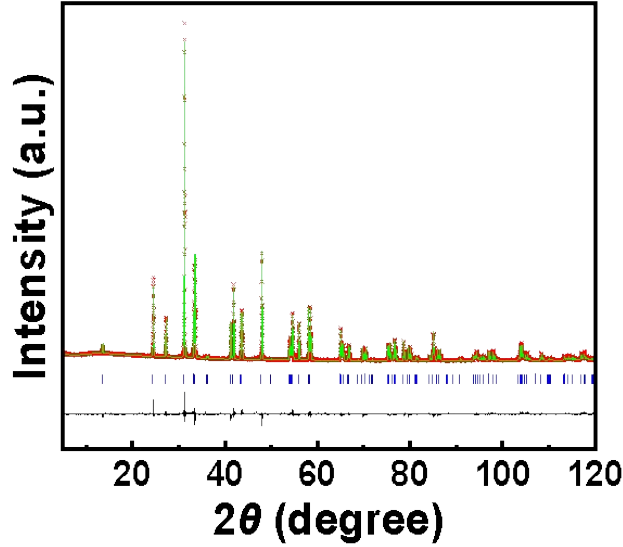


**Figure S9.** Rietveld plot of the X-ray diffraction data of LSKNCO11 at room temperature. The plus symbol represents the observed value, the solid line represents the calculated value, the marks below the diffraction patterns are the calculated reflection positions, and the difference curve is shown at the bottom in the figure.

## 2. Rietveld refinement details for LSKNCO1, LSKNCO2, LSKNCO3, LSKNCO4, LSKNCO6, LSKNCO7, LSKNCO8, LSKNCO10, and LSKNCO11.

Usually, the Rietveld refinement results shown in the Tables should be carefully discussed for a new structure. However, the structure of the samples LSKNCO1 to LSKNCO7 is the same as LSKNCO1, which is  $\text{La}_{1.75}\text{Sr}_{0.25}\text{CuO}_{4-\delta/4}$ . The structure of  $\text{La}_{1.75}\text{Sr}_{0.25}\text{CuO}_{4-\delta/4}$  has been discussed by J. B. Goodenough et al. (J. B. Goodenough, J. S. Zhou and K. Allan, *J. Mater. Chem.* 1991, 1, 715-724). The data shown in Table 1 (for LSKNCO5), Table S1 (for LSKNCO2), Table S2 (for LSKNCO1, LSKNCO3, and LSKNCO4), and Table S3 (for LSKNCO6, and LSKNCO7) are wanted to let the readers to know how similar is the structure of the samples LSKNCO1 to LSKNCO7 with the structure of  $\text{La}_{1.75}\text{Sr}_{0.25}\text{CuO}_{4-\delta/4}$  reported by J. B. Goodenough et al. Similarly, the structure of the samples LSKNCO8 to LSKNCO11 is the same as that of  $\text{La}_2\text{CuO}_{4-\delta}$ , which has been reported by M. Onoda et al. (M. Onoda, S. Shamoto, M. Sato and S. Hosoya, *Jpn. J. Appl. Phys.*, 1987, 26, L363-L365.). The data shown in Table 1 (for LSKNCO9) and Table S4 (for LSKNCO8, LSKNCO10, and LSKNCO11) are to show the similarity of the structure of the samples LSKNCO8 to LSKNCO11 with the structure of  $\text{La}_2\text{CuO}_{4-\delta}$ . Repeated descriptions of the structures are omitted. One can reference the work of J. B. Goodenough et al. and/or the work of M. Onoda et al. for the details on the structure of  $\text{La}_{1.75}\text{Sr}_{0.25}\text{CuO}_{4-\delta/4}$  and/or  $\text{La}_2\text{CuO}_{4-\delta}$ .

**Table S1.** Rietveld refinement details of the  $\text{La}_{7+2x}\text{Sr}_{1-4x}\text{K}_x\text{Na}_x\text{Cu}_4\text{O}_{16-\delta}$  samples with  $x = 0.025$  (space group:  $I4/mmm$ ).

Sample	$x = 0.025$ , LSKNCO2
Lattice Parameters (Å)	$a=b=3.7729(4)$ , $c=13.2638(6)$
Volume (Å <sup>3</sup> )	188.810(2)
Atom	(x, y, z)
La/Sr/K/Na <sup>a</sup>	0,0,0.3601(3)
Cu1	0,0,0
O1	0,1/2,0
O2	0,0,0.1819(7)
$B_{eq}(La/Sr/K/Na)(\text{Å}^2)^b$	0.8057(7)
$B_{eq}(Cu)$ (Å <sup>2</sup> )	1.0737(8)
$B_{eq}(O1)$ (Å <sup>2</sup> )	0.7056(7)
$B_{eq}(O2)$ (Å <sup>2</sup> )	1.6422(5)
R factor <sup>c</sup>	$R_{wp}^x = 0.042$ , $R_{wp}^n = 0.068$

<sup>a</sup>The occupancy of La/Sr/K/Na is 0.881250:0.112500:0.003125:0.003125 for  $x = 0.025$ .

<sup>b</sup> $B_{eq}$  is the thermal displacement parameter.

<sup>c</sup> $R_{wp}^x$  and  $R_{wp}^n$  are the weighted R factors calculated by  $(\sum(w(I_0-I_c)^2)/\sum(w(I_0^2)))^{0.5}$  for powder X-ray and neutron diffraction data, respectively;  $R_p^x$  and  $R_p^n$  are the R factors calculated by  $(\sum(|I_0-I_c|)/\sum(I_0))$  for powder X-ray and neutron diffraction data, respectively.

**Table S2.** Rietveld refinement details of the  $La_{7+2x}Sr_{1-4x}K_xNa_xCu_4O_{16-\delta}$  samples with  $x = 0.000$ ,  $x = 0.050$  and  $x = 0.075$  (space group:  $I4/mmm$ ).

Sample	$x = 0.000$ , LSKNCO1	$x = 0.050$ , LSKNCO3	$x = 0.075$ , LSKNCO4
Lattice Parameters (Å)	$a=b=3.7703(4)$ , $c=13.2616(9)$	$a=b=3.7737(6)$ , $c=13.2519(5)$	$a=b=3.7765(3)$ , $c=13.2519(3)$
Volume (Å <sup>3</sup> )	188.514(2)	188.723(2)	188.998(1)
Atom	(x, y, z)	(x, y, z)	(x, y, z)
La/Sr/K/Na <sup>a</sup>	0,0,0.3602(3)	0,0,0.3606(3)	0,0,0.3606(3)
Cu1	0,0,0	0,0,0	0,0,0
O1	0,1/2,0	0,1/2,0	0,1/2,0
O2	0,0,0.184	0,0,0.184	0,0,0.184
$B_{eq}(La/Sr/K/Na)(\text{Å}^2)^b$	0.7885(3)	0.9293(1)	0.7822(7)
$B_{eq}(Cu)$ (Å <sup>2</sup> )	1.0575(8)	1.3288(8)	1.3973(4)
$B_{eq}(O1)$ (Å <sup>2</sup> )	1	1	1
$B_{eq}(O2)$ (Å <sup>2</sup> )	1	1	1

	$R_{wp}^x = 0.040,$	$R_{wp}^x = 0.044,$	$R_{wp}^x = 0.044,$
R factor <sup>c</sup>	$R_p^x = 0.029$	$R_p^x = 0.030$	$R_p^x = 0.031$

<sup>a</sup>The occupancy of La/Sr/K/Na is 0.875:0.125:0.000:0.000 for  $x = 0.000$ , 0.88750:0.10000:0.00625:0.00625 for  $x = 0.050$  and 0.893750:0.087500:0.009375:0.009375 for  $x = 0.075$ .

<sup>b</sup> $B_{eq}$  is the thermal displacement parameter.

<sup>c</sup> $R_{wp}^x$  is the weighted R factors calculated by  $(\sum(w(I_0-I_c)^2)/\sum(w(I_0^2)))^{0.5}$  for powder X-ray diffraction data;  $R_p^x$  is the R factors calculated by  $\sum(|I_0-I_c|/\sum(I_0))$  for powder X-ray diffraction data.

**Table S3.** Rietveld refinement details of the  $La_{7+2x}Sr_{1-4x}K_xNa_xCu_4O_{16-\delta}$  samples with  $x = 0.125$  and  $x = 0.150$  (space group:  $I4/mmm$ ).

Sample	$x = 0.125$ , LSKNCO6	$x = 0.150$ , LSKNCO7
Lattice Parameters (Å)	a=b=3.7806(1), c=13.2329(6)	a=b=3.7835(2), c=13.2237(8)
Volume (Å <sup>3</sup> )	189.136(1)	189.291(1)
Atom	(x, y, z)	(x, y, z)
La/Sr/K/Na <sup>a</sup>	0,0,0.3611(4)	0,0,0.3612(4)
Cu1	0,0,0	0,0,0
O1	0,1/2,0	0,1/2,0
O2	0,0,0.184	0,0,0.184
$B_{eq}(La/Sr/K/Na)(\text{Å}^2)^b$	0.0233(6)	0.0083(1)
$B_{eq}(Cu)(\text{Å}^2)$	0.5204(6)	0.6964(3)
$B_{eq}(O1)(\text{Å}^2)$	1	1
$B_{eq}(O2)(\text{Å}^2)$	1	1
R factor <sup>c</sup>	$R_{wp}^x = 0.045,$ $R_p^x = 0.030$	$R_{wp}^x = 0.045,$ $R_p^x = 0.030$

<sup>a</sup>The occupancy of La/Sr/K/Na is 0.906250:0.062500:0.015625:0.015625 for  $x = 0.125$  and 0.91250:0.05000:0.01875:0.01875 for  $x = 0.150$ .

<sup>b</sup> $B_{eq}$  is the thermal displacement parameter.

<sup>c</sup> $R_{wp}^x$  is the weighted R factors calculated by  $(\sum(w(I_0-I_c)^2)/\sum(w(I_0^2)))^{0.5}$  for powder X-ray diffraction data;  $R_p^x$  is the R factors calculated by  $\sum(|I_0-I_c|/\sum(I_0))$  for powder X-ray diffraction data.

**Table S4.** Rietveld refinement details of the  $La_{7+2x}Sr_{1-4x}K_xNa_xCu_4O_{16-\delta}$  samples with  $x =$

0.175,  $x = 0.225$  and  $x = 0.250$  (space group: *Fmmm*).

Sample	$x = 0.175$ , LSKNCO8	$x = 0.225$ , LSKNCO10	$x = 0.250$ , LSKNCO11
Lattice Parameters (Å)	a=5.3512(1), b=5.3602(3), c=13.2082(1)	a=5.3559(5), b=5.3892(6), c=13.1814(4)	a=5.3565(2), b=5.3977(3), c=13.1631(4)
Volume (Å <sup>3</sup> )	378.856(3)	380.472(3)	380.582(3)
Atom	(x, y, z)	(x, y, z)	(x, y, z)
La/Sr/K/Na <sup>a</sup>	0,0,0.3612(3)	0,0,0.3612(3)	0,0,0.3612(3)
Cu1	0,0,0	0,0,0	0,0,0
O1	1/4,1/4,0	1/4,1/4,0	1/4,1/4,0
O2	0,0,0.18327	0,0,0.18327	0,0,0.18327
$B_{eq}(\text{La/Sr/K/Na})(\text{Å}^2)^b$	1.0369(7)	0.9985(5)	0.9597(2)
$B_{eq}(\text{Cu})(\text{Å}^2)$	1.5682(6)	1.5202(6)	1.6484(8)
$B_{eq}(\text{O1})(\text{Å}^2)$	1	1	1
$B_{eq}(\text{O2})(\text{Å}^2)$	1	1	1
R factor <sup>c</sup>	$R_{wp}^x = 0.042$ , $R_p^x = 0.030$	$R_{wp}^x = 0.045$ , $R_p^x = 0.032$	$R_{wp}^x = 0.043$ , $R_p^x = 0.032$

<sup>a</sup>The occupancy of La/Sr/K/Na is 0.918750:0.037500:0.021875:0.021875 for  $x = 0.175$ , 0.931250:0.012500:0.028125:0.028125 for  $x = 0.225$  and 0.93750:0.00000:0.03125:0.03125 for  $x = 0.250$ .

<sup>b</sup> $B_{eq}$  is the thermal displacement parameter.

<sup>c</sup> $R_{wp}^x$  is the weighted R factors calculated by  $(\sum(w(I_0 - I_c)^2) / \sum(w(I_0^2)))^{0.5}$  for powder X-ray diffraction data;  $R_p^x$  is the R factors calculated by  $\sum(|I_0 - I_c| / \sum(I_0))$  for powder X-ray diffraction data.

### 3. Comparison of the lattice parameters of $\text{La}_{7+2x}\text{Sr}_{1-4x}\text{K}_x\text{Na}_x\text{Cu}_4\text{O}_{16-\delta}$

The changes in lattice parameters of  $\text{La}_{7+2x}\text{Sr}_{1-4x}\text{K}_x\text{Na}_x\text{Cu}_4\text{O}_{16-\delta}$  compared to the  $\text{La}_{2-x}\text{Sr}_x\text{Cu}_4\text{O}_{16-\delta}$  ( $0.1 \leq x \leq 0.25$ ) system further support the idea that  $\text{K}^+$  and  $\text{Na}^+$  are substituting  $\text{Sr}^{2+}$  at the La/Sr sites<sup>26</sup>, as shown in Figure S10. To facilitate the comparison, we represented the chemical formulas of the two systems as  $\text{La}_{7.5-0.5y}\text{Sr}_y\text{K}_{0.25-0.25y}\text{Na}_{0.25-0.25y}\text{Cu}_4\text{O}_{16-\delta}$  and  $\text{La}_{8-y}\text{Sr}_y\text{Cu}_4\text{O}_{16-\delta}$  ( $0 \leq y \leq 1$ ), respectively. If no K or Na exists in the  $\text{La}_{7.5-0.5y}\text{Sr}_y\text{K}_{0.25-0.25y}\text{Na}_{0.25-0.25y}\text{Cu}_4\text{O}_{16-\delta}$  samples, they can be noted as  $\text{La}_{7.5-0.5y}\text{Sr}_y\text{Cu}_4\text{O}_{16-\delta}$ . There should be more vacancies at La site in  $\text{La}_{7.5-0.5y}\text{Sr}_y\text{Cu}_4\text{O}_{16-\delta}$  compared to the  $\text{La}_{8-y}\text{Sr}_y\text{Cu}_4\text{O}_{16-\delta}$  samples when  $y < 1$ . We would expect the unit cell volume of  $\text{La}_{7.5-0.5y}\text{Sr}_y\text{Cu}_4\text{O}_{16-\delta}$  should be smaller than that of  $\text{La}_{8-y}\text{Sr}_y\text{Cu}_4\text{O}_{16-\delta}$  due to the greater number of

vacancies. However, our experimental results show that the unit cell volume of our samples is actually larger than that of  $\text{La}_{8-y}\text{Sr}_y\text{Cu}_4\text{O}_{16-\delta}$ . This observed increase in volume strongly supports  $\text{K}^+$  and  $\text{Na}^+$  should occupy the La sites, as these larger ions expand the lattice.

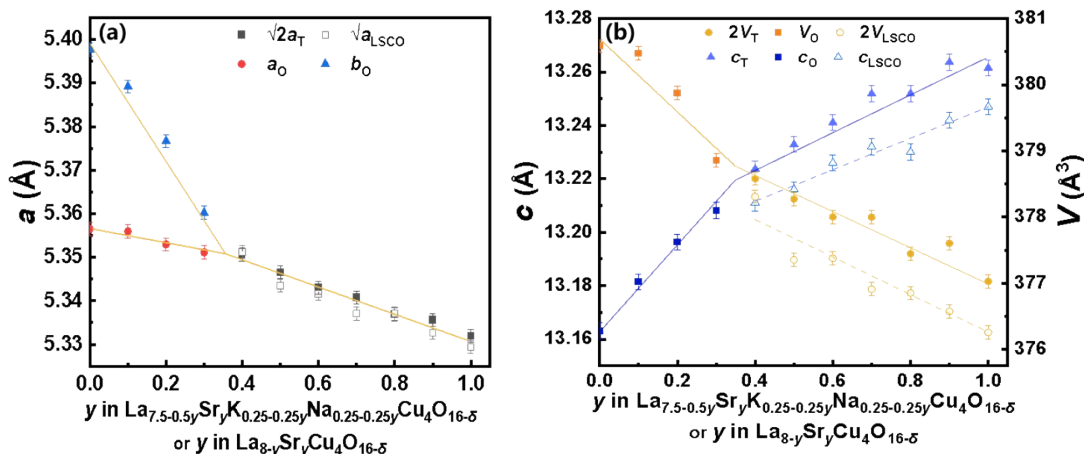


**Figure S10.** Lattice parameters of  $\text{La}_{7.5-0.5y}\text{Sr}_y\text{K}_{0.25-0.25y}\text{Na}_{0.25-0.25y}\text{Cu}_4\text{O}_{16-\delta}$  and  $\text{La}_{8-y}\text{Sr}_y\text{Cu}_4\text{O}_{16-\delta}$  ( $0 \leq y \leq 1$ ).  $a_T$ ,  $c_T$ ,  $V_T$ , the lattice parameter  $a$ ,  $c$ , and the volume of unit cell for the tetragonal phase of  $\text{La}_{7.5-0.5y}\text{Sr}_y\text{K}_{0.25-0.25y}\text{Na}_{0.25-0.25y}\text{Cu}_4\text{O}_{16-\delta}$ ;  $a_o$ ,  $b_o$ ,  $c_o$ ,  $V_o$ , the lattice parameter  $a$ ,  $b$ ,  $c$ , and the volume of unit cell for the orthogonal phase of  $\text{La}_{7.5-0.5y}\text{Sr}_y\text{K}_{0.25-0.25y}\text{Na}_{0.25-0.25y}\text{Cu}_4\text{O}_{16-\delta}$ ;  $a_{LSCO}$ ,  $c_{LSCO}$ ,  $V_{LSCO}$ , the lattice parameter  $a$ ,  $c$ , and the volume of unit cell of  $\text{La}_{8-y}\text{Sr}_y\text{Cu}_4\text{O}_{16-\delta}$  ( $0 \leq y \leq 1$ ).

#### 4. Energy-dispersive X-ray spectroscopy

The La: Sr: K: Na: Cu ratio of LSKNCO9 and the La: K: Na: Cu ratio of LSKNCO11 is 27.88: 0.68: 0.76: 0.82: 15.76 and 28.23: 0.82: 0.94: 14.70, respectively, which are essentially identical to their ideal values and evidence that the chemical composition of the samples aligns with the planned formula. However, we acknowledge that for samples with lower doping levels, obtaining detailed and accurate data can be challenging due to the limitations in the sensitivity and precision of the EDX instrument. Despite these limitations, the data we have collected from samples with higher doping levels (LSKNCO9 and LSKNCO11) strongly suggest that our synthesis process effectively controls the composition to match the intended stoichiometry across the entire series.

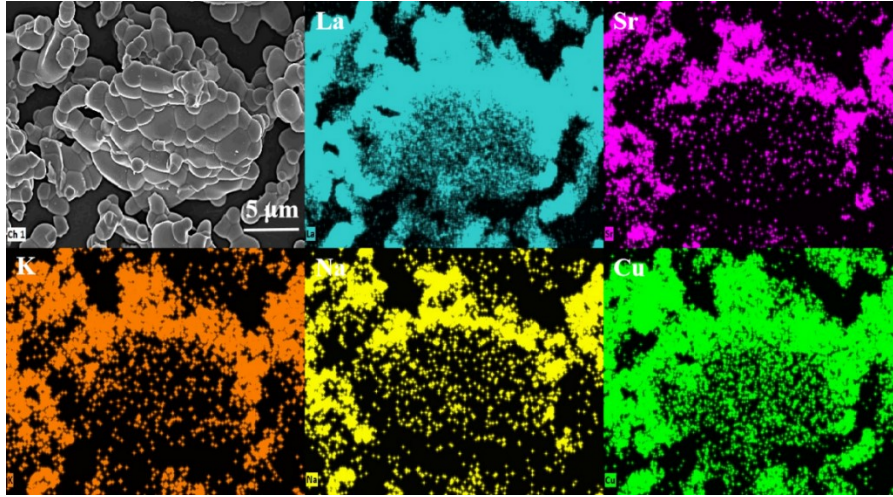


Figure S11. Energy-dispersive X-ray spectroscopy of the LSKNCO9 sample.

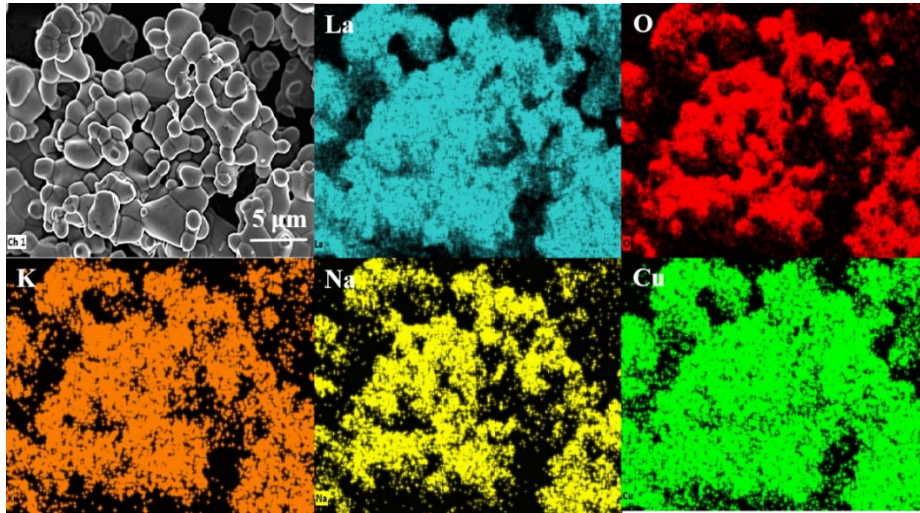


Figure S12. Energy-dispersive X-ray spectroscopy of the LSKNCO11 sample.

#### 4. The configurational entropy for $\text{La}_{7+2x}\text{Sr}_{1-4x}\text{K}_x\text{Na}_x\text{Cu}_4\text{O}_{16-\delta}$ .

**Table S5.** The configurational entropy for  $\text{La}_{7+2x}\text{Sr}_{1-4x}\text{K}_x\text{Na}_x\text{Cu}_4\text{O}_{16-\delta}$  samples with  $x = 0.0, 0.025, 0.05, 0.075, 0.10, 0.125, 0.15, 0.175, 0.20, 0.225$  and  $0.25$ .

Sample	$x = 0.000$	$x = 0.025$	$x = 0.050$	$x = 0.075$	$x = 0.100$	$x = 0.125$
$S_{ss}^{config}$	8.840	8.880	8.895	8.898	8.893	8.878
	$x = 0.150$	$x = 0.175$	$x = 0.200$	$x = 0.225$	$x = 0.250$	
$S_{ss}^{config}$	8.854	8.820	8.775	8.711	8.604	

#### 5. Temperature-dependent resistance and magnetic susceptibility of $\text{La}_{7+2x}\text{Sr}_{1-4x}\text{K}_x\text{Na}_x\text{Cu}_4\text{O}_{16-\delta}$ .

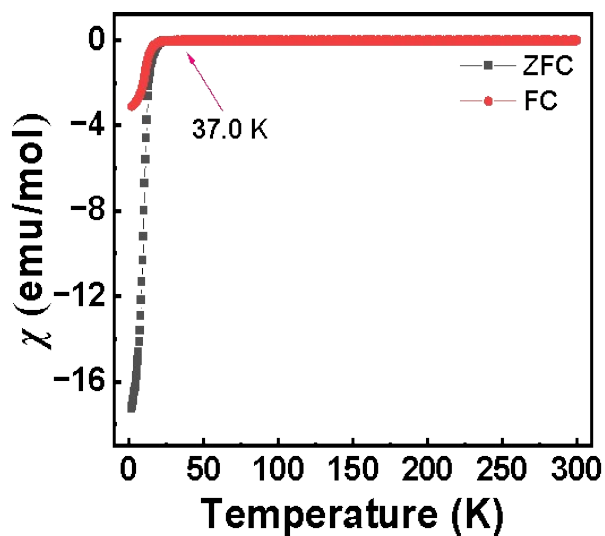


Figure S13. Temperature dependence of DC magnetic susceptibility of LSKNCO1.

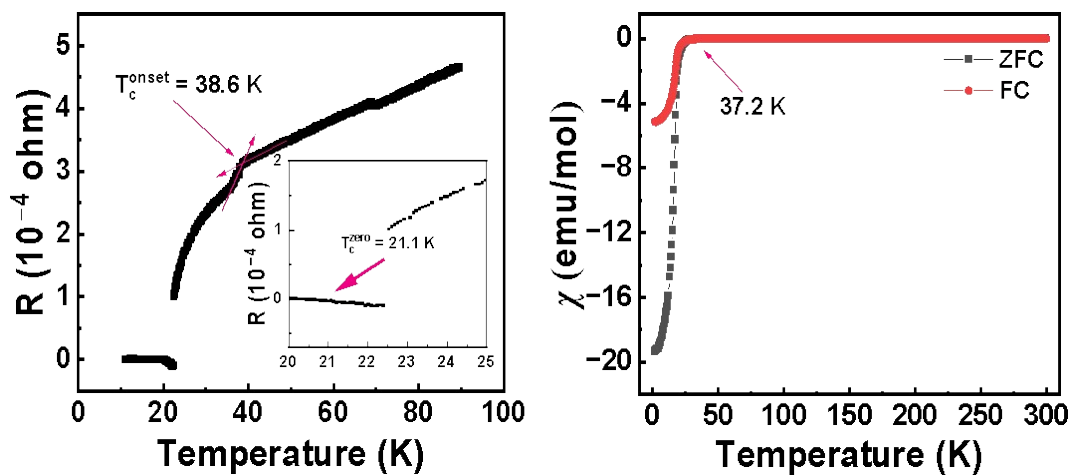


Figure S14. Temperature-dependent resistance and magnetic susceptibility of LSKNCO2.

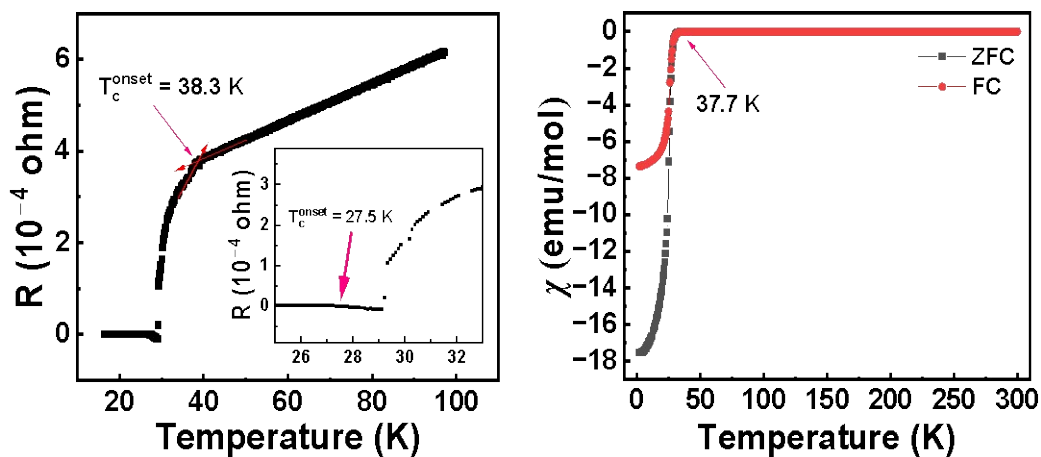


Figure S15. Temperature-dependent resistance and magnetic susceptibility of LSKNCO3.

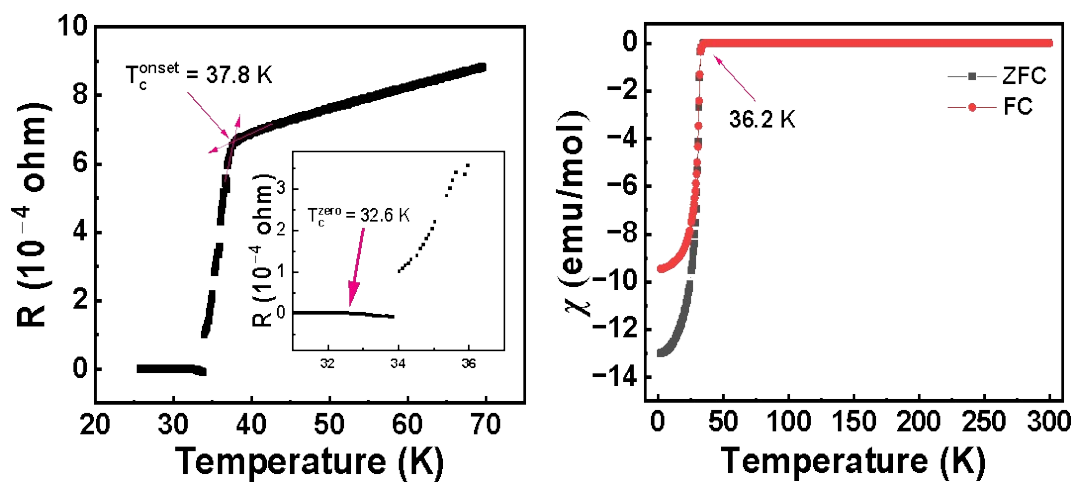


Figure S16. Temperature-dependent resistance and magnetic susceptibility of LSKNCO4.

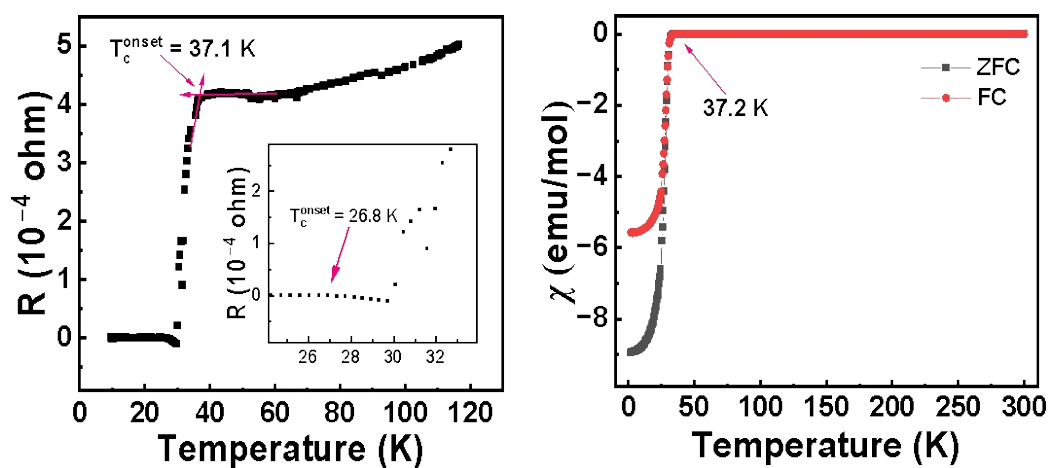


Figure S17. Temperature-dependent resistance and magnetic susceptibility of LSKNCO6.

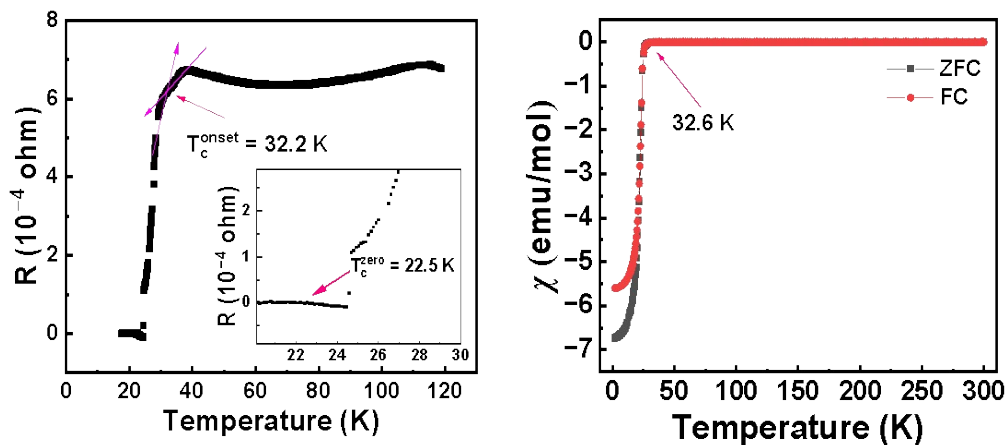


Figure S18. Temperature-dependent resistance and magnetic susceptibility of LSKNCO7.

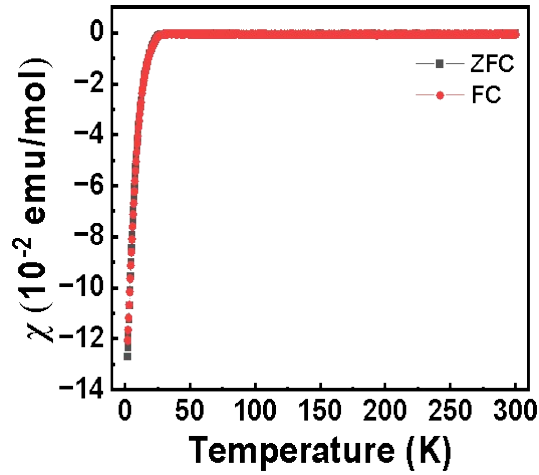


Figure S19. Temperature dependence of DC magnetic susceptibility of LSKNCO9.

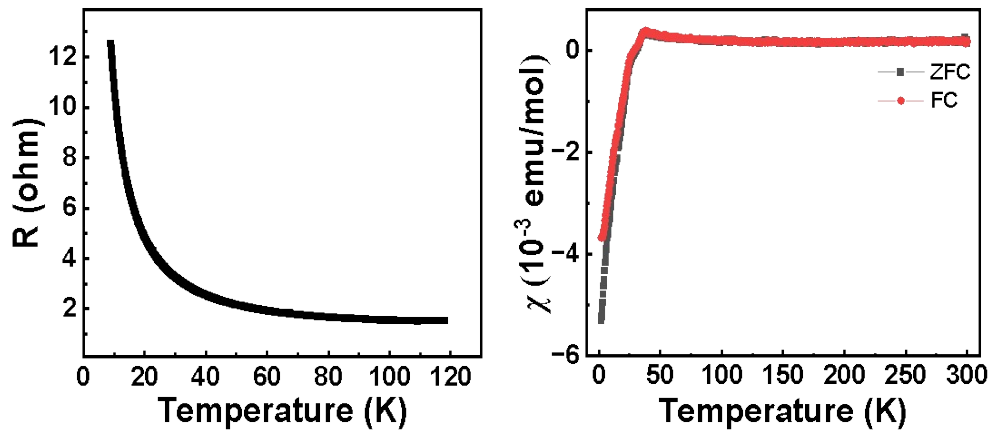


Figure S20. Temperature-dependent resistance and magnetic susceptibility of LSKNCO10.

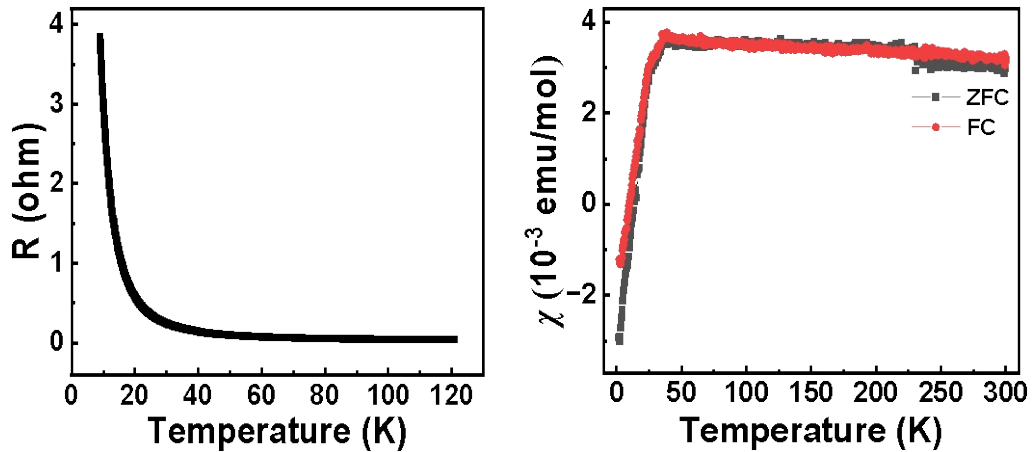


Figure S21. Temperature-dependent resistance and magnetic susceptibility of LSKNCO11.